Pipe diffusion ripening of Si precipitates in Al-0.5%Cu-1%Si thin films

Marc Legros, Belkhiri Kaouache, Patrice Gergaud, Olivier Thomas, Gerhard Dehm, John Balk, Eduard Arzt

Pipe diffusion ripening of Si precipitates in Al-0.5%Cu-1%Si thin films

Journal:	*Philosophical Magazine & Philosophical Magazine Letters*
Manuscript ID:	TPHM-05-Feb-0043.R2
Journal Selection:	Philosophical Magazine
Date Submitted by the Author:	30-May-2005
Complete List of Authors:	Legros, Marc; CEMES-CNRS, MC2 Kaouache, Belkhiri; ENSAM, LPMM Gergaud, Patrice; Université Saint Jerome, TECSEN Thomas, Olivier; Université Saint Jerome, TECSEN Dehm, Gerhard; University of Stuttgart, Max Planck Institut fur Metallkunde Balk, John; University of Kentucky, Chemical and materials engineering Arzt, Eduard; University of Stuttgart, Max Planck Institut fur Metallkunde
Keywords:	thin films, TEM, dislocations, diffusion, precipitation
Keywords (user supplied):	

Pipe diffusion ripening of Si precipitates in Al-0.5%Cu-1%Si thin films

M. Legros°, B. Kaouache*, P. Gergaud†, O. Thomas†, G. Dehm¥, T.J. Balk‡ and E. Arzt¥

°*CEMES-CNRS, 29 rue Jeanne Marvig, 31055 Toulouse -France*

**LPMM, ENSAM, Technopole, 4 rue Augustin Fresnel, 57078 Metz*

† *Laboratoire TECSEN, Faculté des Sciences de St Jerôme, 13397 Marseille -France*

¥ *Max-Planck-Institute for Metals Research and Institut für Metallkunde, University of Stuttgart Heisenbergstr. 3, 70569 Stuttgart - Germany*

‡ *Dept. Chem. and Mat. Eng., University of Kentucky, Lexington, KY 40506 -USA*

ABSTRACT

Al-0.5%Cu-1%Si thin films deposited onto oxidized Si substrates were subjected to both wafer curvature and *in situ* transmission electron microscopy (TEM) thermal cycling experiments between room temperature and 450°C. The evolution of precipitates was monitored during cycling. Chemical analysis revealed that the precipitates are pure Si. Their average size increased from 80 nm in the as-deposited state to 300 nm after thermal cycling. Si precipitates serve as anchoring points for dislocations and grain boundaries. Direct evidence for pipe-diffusion ripening was found in the vicinity of a dissolving precipitate. Real-time measurement of the radius of the precipitate allowed us to estimate the coefficient of pipe diffusion of Si in Al at this temperature. As expected, this coefficient is several orders of magnitude larger than the volume diffusion coefficient. The impact of precipitate ripening on the mechanical behaviour of these alloyed Al films will also be discussed.

§1. INTRODUCTION

Al-0.5%Cu-1%Si is one of the most widely used Al alloys for interconnects in integrated circuits. Addition of Cu and Si has been found to reduce electromigration [1] and diffusion from the substrate, respectively. In devices, these films are subjected to stresses that arise mainly from differential thermal expansion of the metal film and the underlying oxidized Si substrate. These stresses, coupled with temperature, induce changes in the as-deposited (out of equilibrium) structure of the film[2, 3]. To investigate the mechanical response of metallic films on rigid substrates, thermal stress cycles are commonly performed using laser profilometry [4, 5] or X-ray diffraction [6-8] to determine the stress in the film. Various aspects of the mechanical behavior of pure and alloyed Al films have been studied for more than 20 years, and alloying elements have been proven to dramatically change the mechanical behavior of these films [4, 9, 10]. However, in small scale systems, where the diffusion paths are short and where stresses can be very localized, the interplay between dislocations, solute atoms and precipitates is not clear [11, 12].

° Corresponding author : legros@cemes.fr

The plastic deformation of thin metallic films submitted to thermal cycles is considered by many authors to be governed by dislocations processes e.g. [13, 14]. From this point of view, the high yield stresses and hardening rates observed in thin films are explained by the motion of dislocations that interact elastically with the substrate or other dislocations as found e.g. in epitaxial films [15]. On the other hand, recent cross-sectional *in situ* experiments on polycrystalline Al films demonstrated that, among successive cycles, the contribution of dislocations to the plastic deformation is significant only during the first one[16, 17] Here, we would like to emphasize the capacity of dislocations to act as fast diffusion paths, similar to grain boundaries [18, 19]. Such diffusion processes are known to influence thin film plasticity [16, 20-22]. The effects of dislocations and grain boundaries on diffusion are often determined indirectly [23, 24], although some direct evidence was recently found in gold films on SiC [25]. In Al/Si thin films, pipe diffusion has been put forward to explain the apparent increase of the diffusion coefficient of Si in Al [26, 27] as compared to the bulk value.

Deleted:

In the present work, we have characterized the intra- and intergranular precipitates found in polycrystalline Al-0.5%Cu-1%Si films and observed their evolution throughout thermal cycles using both *post mortem* and *in situ* transmission electron microscopy (TEM). Monitoring the rapid dissolution of a precipitate in contact with a dislocation offers the possibility to calculate directly the coefficient of pipe diffusion of Si in Al. Finally, the interaction between dislocations and precipitates will be discussed in order to shed light on the mechanical behaviour of these films.

§2. Experimental Details

Al-0.5%Cu-1%Si (hereafter named Al(Si,Cu)) films with a thickness of 550 nm were deposited at 450°C onto oxidized 6" (001) Si wafers by magnetron sputtering. After film deposition, the thickness of the wafers was reduced by mechanical and chemical back polishing from 680 µm to 180 µm. Rectangular pieces (10 x 20 mm) were cleaved from the as-deposited wafer and were cycled from 20 to 450°C in a 10^{-6} Torr vacuum at 10K/min. During the cycles, stress was monitored using wafer curvature measurements [28]. The stress evolution in function of temperature has been reported and discussed elsewhere [16].

Cross-section TEM samples for *in situ* and *post mortem* observations were prepared using tripod polishing [17]. This preparation technique was also utilized for plan view specimen preparation. The thinning procedure was kept identical for both as-deposited and cycled samples, so the observed microstructural evolution can be ascribed to temperature and stress only. We performed *in situ* TEM experiments in a JEOL 2000FX microscope, and *post mortem* studies in a JEOL 2010 or a Philips CM200 equipped with energy-dispersive X-ray spectroscopy (EDS) detector for chemical analysis. All TEM studies were performed at an accelerating voltage of 200kV.

Deleted: l

§3. Results

Fig. 1 presents plan view TEM micrographs taken before and after four thermal cycles of an Al(Si,Cu) film. As can be seen in figure 1(a), precipitates are initially homogeneously distributed. Most of them lie inside the grains, although some sit at grain boundaries. From the cross-section images in figures 3 and 4 (in situ sequence), it is also clear that these

precipitates are located away from the free surface of the film and from the Al/SiO_x interface. Thermal cycling causes their average diameter to grow from 80 nm in the as-deposited state (figure 1a) to 300nm after cycling (figures 1c,d). Note that most of the precipitates remain intragranular during growth and that many dislocations are attached to them, both before and after the cycles.

To determine the nature of these precipitates, we performed both chemical (figure 2) and micro-diffraction (figure 3) analysis on cycled cross-sectional specimens. Figure 2(a) shows the EDS signal collected in an Al region with no precipitate. The TEM was set in nano-probe mode so that the investigated section was of the order of the electron probe itself. Figure 2(b) corresponds to a similar spectrum acquired from the precipitate seen in figure 3 and clearly indicates the presence of Si while the Al and Cu peaks remain unchanged. The enhanced presence of Cu (in equivalent amount on both spectra) is thought to arise from the TEM Cu grid that supports the cross sectional sample. Quantitative analysis of the spectrum of figure 2(b) leads to a Si content of about 10-15 wt%. Considering the thickness of the Al layer at this location (between 400 and 500 nm), the proportion of Si should be close to 20-30%, assuming the precipitate to be of pure Si and globular. However, unless carefully calibrated, EDS measurements are mostly qualitative. To verify the nature of these precipitates we performed micro-diffraction and dark field imaging. Part of these observations is reported in figure 3. The spot patterns obtained from the precipitate clearly match the interplanar distances of diamond cubic silicon while those from the Al matrix served as reference. Figures 3(a) and 3(b) were captured using respectively $g=111_{Si}$ and $g= 131_{Si}$; figure 3(c) is the corresponding stereographic projection of the Si precipitate. In figure 3(b), a twinned region is visible in the middle of the precipitate. Figure 3(d), where only this twinned region is in contrast, is obtained by selecting a diffracting vector $g=-11-1_{Si}$ that does not pertain to the Si precipitate. The orientation of this twinned region is given in figure 3(e). The twinning plane is (111). This plane also corresponds to the coinciding plane between the Al matrix and the Si precipitate and to the interfacial plane of the Al grain with the SiOx layer covering the substrate. The orientation of the Al grain containing the Si precipitate is given in figure 3(g) and the corresponding dark field image obtained using $g=-111_{Al}$ is shown in figure 3(f). In this micrograph, the right and left sides of the Al grain are in contrast while the precipitate is out of contrast. The strong difference between the contrast of the sides and the center part of the grain comes from the small deviation to Bragg conditions used to capture picture 3f. From these different stereographic projections, a tentative match between the directions of the Al matrix and the Si grains along the (111) plane gives $<123>_{Si}$ // $<110>_{Al}$. The resulting lattice mismatch amounts to 0.74%, which is reasonably low.

Deleted: bright

In situ TEM allowed the evolution of Si precipitates to be monitored. Their ripening is usually not fast enough to be grabbed on video in a reasonable time. However, in the case of pipe diffusion, this time was considerably lowered. Figure 4 displays a sequence of video frames showing the dissolution of a small precipitate (noted A) in favor of a larger one (noted C). This was observed at the end of a heating ramp from 20 to 450°C. Dislocation 1 has one end attached to the Si precipitate labeled C and moves toward the Al/SiOx interface in figure 4 (a). Between figures 4 (b) and (c), dislocation 1 anchors on the Si precipitate labeled A and forms a link between A and C ; the left end of dislocation 1 ends on a free surface of the foil. Note that the dislocation line contrast disappears on precipitate A between figures (b) and (c). From figure (d) to (e), precipitate A disappears but the pinning point on dislocation 1 is still visible in figure 4(e). In figure 4(f), dislocation 1 is released under low stress (the local stress change may be due to the back up of dislocation 6), indicating that the precipitate is completely dissolved. Figure 4(g) schematically represents the microstructure from figure 4(a) to (f).

The radius and volume evolution for precipitates A and C are represented in figure 5(a) and (b), respectively. The resolution from the video frame leads to an error bar of about ±5 nm on the value of the radius r_A of precipitate A. Since the total volume V_{tot} of precipitates A and C should be constant during the dissolution of A, it is possible to calculate at each time the radius r_C of precipitate C, as presented on plot 5(a) :

$$r_C = \left[\frac{3V_{tot}}{4\pi} - r_A^3 \right]^{\frac{1}{3}} \quad [1]$$

The total calculated change of r_C does not exceed 5 nm, which is within the resolution of the video frames. This finding is compatible with the fact that no significant growth of C is visible from the pictures 4(a) to (f). Since we know the volume evolution of both precipitates, we can calculate the coefficient D_p of pipe diffusion through dislocation 1:

$$J_p = \frac{-D_p}{\Omega k T} \nabla \mu = \frac{-D_p}{\Omega k T} \frac{\Delta \mu}{\Delta l} \quad [2]$$

where J_p is the flux of Si atoms, Ω the atomic volume of silicon, k Boltzmann's constant , T the temperature, and Δμ the difference of chemical potential between precipitates A and C. Δl is the distance between the two precipitates; here, Δl = 250 nm.

On the other hand, J_p is simply given by writing the number of atoms transferring from precipitate A to precipitate C :

$$J_P = \frac{dV}{dt} \frac{1}{\Omega s_p} \quad [3]$$

where V can be either $-V_A$ or V_C, (because $V_A+V_C = V_{tot} = 97500$ nm^3 =constant) and s_p is the cross-sectional area of the pipe. As discussed later, this last parameter is not known, but is usually considered as a disk with a radius equal to the Burgers vector of the dislocation connecting the precipitates [29]. For a perfect dislocation in Al, $s_p = 0.25$ nm^2. In the present case of Ostwald ripening, the driving force for coalescence is the reduction of the total interfacial energy of precipitates A and C. The resulting difference of chemical potential can be written (e.g. [30]):

$$\Delta \mu = 2\Omega\gamma \left(\frac{1}{r_A} - \frac{1}{r_C} \right) \quad [4]$$

where γ is the surface energy of the precipitate. As r_A decreases, the driving force for diffusion Δμ increases. Combining equations [2] to [4] leads to an expression for D_p :

$$D_p = \frac{kT}{2\Omega\gamma s_p} \frac{dV}{dt} \left[\frac{1}{r_C} - \frac{1}{r_A} \right]^{-1} \Delta l \quad [5]$$

The volume variation dV/dt as a function of time was calculated for precipitate A every 10 s during the pipe diffusion process, and was approximated as [V(t+10)-V(t)]/10. Here, dV/dt ranges between 700 and 2500 nm^3/s but, as seen in figure 5(b), V(t) can be fairly well approximated by a linear curve with a slope of 1500 nm^3/s which is the average value of dV/dt. For Si, Ω equals 0.02 nm^3 and γ has been taken as the surface energy of {111} planes, that is 1.4 J/m^2 [31]. Inserting these values into equation [5] leads to a pipe diffusion

Deleted:

coefficient D_p ranging between 2 and 24 x10^{-8} cm^2/s. The scatter around the median value of 11 x 10^{-8} cm^2/s comes from the error bar on the measurement of r_A on the video frames and will be discussed in the next section. This value of D_P is about 400 times larger than the coefficient of diffusion $D_{Si\text{-}Al}$ of Si in the bulk Al alloy at 450°C : $D_{Si/Al}$ (450°C) = 3x10^{-10} cm^2/s [32, 33]. Qualitatively, the fact that pipe-diffusion is much more efficient than volume diffusion explains why the dissolution of precipitate A was noticeable among other small precipitates that seem unchanged (see precipitate B in figure 4).

§4. DISCUSSION

Direct observation of pipe-diffusion mechanism has allowed us to calculate the diffusion coefficient of Si in Al through a dislocation. To do so, we have made the following hypothesis:

- The total volume of precipitates A and C is constant during the dissolution of A. This assumption is supported by the fact that no diffusion toward the surface or the interface was observed and that most of the solute Si atoms sit in precipitates. However, van Gurp [27] has observed an unexpected precipitation of Si at the Al/SiO_x interface. We have assumed that this interface was not an easy precipitation location since precipitates connected to it through dislocations (see precipitate B in figure 3) do not dissolve, or at a pace that was not detectable in our experiments. In brief, when precipitates were simultaneously connected through dislocations to the free surface, the Al/SiO_x interface and to another precipitate, diffusion was only observable between precipitates. This does not rule out other diffusion paths, but indicates that precipitate to precipitate pipe-diffusion is the most efficient.

- The pipe section s_P, corresponding to a perfect dislocation in Al, has a radius of one Burgers vector. This assumption, very hard to verify experimentally [34], is commonly used in the literature (for a review, see [29]). The fact that perfect dislocations in Al have a very compact core strengthens this assumption, but slight variations of s_P have a strong impact on D_p, making the precise determination of D_p complex. Nonetheless, the present *in situ* study gives direct values of the atomic flux. In recent atomic calculations in Al-Mg alloys, Picu and Zhang [35] showed that, depending on the dislocation character and core structure, the diffusion path can be as wide as 2.4 nm but is always confined between two adjacent {111} planes. According to these calculations, the most probable diffusion path would have a 1 nm width, which leads to a rectangular "pipe" cross-section of 0.234 nm^2, very close to the value used in this work. .

- The Al-Si interfacial energy has been taken as the surface energy of Si {111} planes. Other authors have considered a value of 1 J/m^2 [36], which is about 40% lower than the value used in this study. The anisotropy of the surface energy of Si and Al has also been neglected. The smaller and rounder the precipitates (such as the ones in figure 4), the more reasonable this assumption. It may become inappropriate in the case of large, faceted precipitates, such as the one in figure 3.

- The effect of stress has been neglected here. Wafer curvature experiments indicate that thermal stresses originating from the difference in CTE between the metallic film and the Si substrate are very low at this temperature [28]. Stresses are even lower in the

Formatted

cross-sectional TEM sample as revealed by the low curvature of the dislocations in figure 4.

- Equation [4] only takes in account surface energies, but growing and shrinking precipitates can also experience variations of their volume strain energy. This second contribution is usually smaller than the surface energy variation, but could be significant here, depending on the nature of the Si/Al interface.
- Because the pipe diffusion mechanism was obviously much faster than volume diffusion, we have also neglected the Ostwald ripening of precipitate C through volume diffusion. It is worth noting that the classic treatment of this mechanism, based on solute atom concentration gradients, (see, for instance [30]) addresses precipitate populations and not individual entities.

Finally, most of the uncertainty in the determination of D_p comes from the inaccuracy in measuring r_A (and r_C) on the video frames. For instance, the fact that dV/dt, and thus the flux of atoms through the dislocation seems constant in spite of an increase of $\Delta\mu$, may be an indication that the diffusion mechanism is the controlling one. Additional experiments are needed to confirm this behavior. Because D_p depends both on the derivative of r^3 (atomic flux density) and on the inverse of $1/r_A$-$1/r_C$ (chemical potential gradient), small errors on r lead to an important scatter on the values of D_p. Two possible ways to enhance r measurements are the use of a better video camera and a lower experimental temperature that would slow down the diffusion process and thus allow the shooting of still pictures. Nevertheless, the present study provides the first direct measurement of the pipe diffusion coefficient measured on a single dislocation and confirms the early assumptions that dislocations act as diffusion short circuits [18, 19, 29, 30]. This result agrees also well with the ratio of 250 between pipe and bulk self diffusion coefficients calculated by Volin et al. [37] using grain boundary diffusion in Al at 450°C. On the other hand, recent calculations seem to indicate that diffusion is not strongly accelerated through dislocations [35]. A more comprehensive comparison between bulk and pipe diffusion would require an Arhenius plot of the pipe diffusion coefficient and therefore additional *in situ* experiments at different temperatures. These experiments are on their way to try to determine the pre-exponential factor and activation energy of pipe diffusion.

We discuss now the role of precipitates on dislocation activity. In the present study, no $\theta(Al_2Cu)$ precipitation has been observed. This may be due to the low concentration of Cu compared to other alloyed thin films, or to the preferential location of these precipitates at grain boundaries and triple junctions [9, 38] The fact that some authors reported θ phase precipitation in the case of Al -0.5% Cu thin films [12] while some others did not [39] has also been attributed to the deposition temperature [12].

The Al_2Cu precursor phases such as θ ' and θ " have similar size and could therefore be difficult to resolve using conventional TEM. They have been observed by Witrouw et al. [12] during thermal cycles of Al-0.5%Cu-1%Si films. Such precipitation has not taken place in our experiments. Because the interaction between dislocations and these nano-scaled phases is strong, *in situ* TEM would have unveiled them. As mentioned earlier, the observed free motion of dislocations between Si precipitates (identical to what is observed in pure Al) is a strong indication of the absence of these (Al,Cu) precursor phases inside the grains.

Formatted: Bullets and Numbering

Deleted: d

Compared to those observed in this study, the grain-like Si precipitates reported by [9] seem very similar in size and shape, but the authors did not discuss intra-granular precipitation. This finding, gathered with the fact that no dissolution of these Si precipitates was observed even at high temperature, is of prime importance regarding the mechanical properties of the alloy film.

In previous work on Al(Si,Cu) films, it has been shown that most of the mobile dislocations were connected to at least one precipitate of Si [16], which can also be observed here in figures 1 and 4. The anchoring efficiency of precipitates becomes larger as they grow and this growth is also accelerated by the pipe diffusion mechanism. As a result of this interplay, the Ostwald ripening of Si precipitates is rapid, which means that their number also decreases rapidly. Consequently, mobile dislocations encounter fewer anchoring sites and these sites are also farther away from each other. Providing a constant or increasing dislocation density, the resulting easier dislocation motion should yield to a reduced strength of the Al(Si,Cu) film as thermal cycling carries on. This is not observed: excepted for a stress bump in compression during the first cycle, the stress/temperature curves of consecutive thermal cycles of Al(Si,Cu) films can be perfectly superimposed [28].

On the other hand, it has been shown that, because of the absence of active sources and the sink effect of the metal/oxide interface, the density of dislocations decreases with successive thermal cycles in pure Al films on oxidized Si substrate [17]. Our observations indicate that the addition of Si precipitates tend to retain some anchored dislocations but do not provide efficient sources to balance the dislocation loss. As a consequence, a decrease of dislocation density is also observed in the present work, supporting the idea of an alternative mode of deformation of the Al(Si,Cu) films.

The phenomenon of the stress bump on as-deposited or relaxed Al(Si,Cu) films has been first explained in terms of dynamic strain aging [28]: solute atoms condensation occurs on dislocation segments during room temperature relaxation, which prevents free glide when the film is strained (heated) again. The stress drop in compression would then correspond to the additional stress needed by the dislocations to overcome this Cottrell atmosphere. The fact that Si precipitates do not dissolve at high temperature and thus do not provide a significant increase of solute atoms concentration does not support this hypothesis. Also, no noticeable change in dislocation mobility, especially at the onset of plasticity (about 150°C) has been reported here nor during previous *in situ* experiments [16]. Alternatively, a grain boundary diffusion mechanism has been put forward to tentatively explain this stress drop [16].

Overall we have observed that a dislocation is an efficient short circuit for diffusion; as dislocations arrays, grain boundaries should have a very similar role. This supports the view that plasticity mediated by diffusional processes [20, 21] can, in some cases, prevail on dislocation glide processes and influence the mechanical behavior of thin metallic films [40].

§5. CONCLUSION

Precipitation in Al -1%Si -0.5%Cu thin films has been documented using *in situ* and *post mortem* TEM observations. Nanoprobe X-ray analysis and microdiffraction indicated that observable precipitates were pure Si and of the intra- or intergranular type. Thermal cycling up to 450°C induced growth of these precipitates from an average size of 80 nm in the as-deposited state to about 300 nm after cycling. This Ostwald ripening was promoted by pipe diffusion, of which a direct and dynamic observation was made for the first time: a single dislocation connecting two Si precipitates caused the rapid dissolution of the smaller in favor

of the larger. From the evolution of the radii, we have calculated the coefficient of pipe diffusion of Si in Al at 450°C.

In Al(Si,Cu) films, pipe diffusion is thought to be a very effective mechanism because :

- Si precipitates proved strong anchoring points for dislocations and grain boundaries, which means that most dislocations are connected to at least one precipitate,
- The coefficient of pipe diffusion at 450°C was estimated about 400 times larger than the coefficient of bulk diffusion for Si in Al at the same temperature.

No Al_2Cu precipitation was observed and the free motion of dislocations between Si precipitates suggests that Al grains are free of the precursor phases too. These combined observations seem to rule out a possible dynamic strain aging in the mechanical behavior of these films. Successive cycling causes the reduction of the number of precipitates and as a consequence the decrease of the dislocation density.

ACKNOWLEDGEMENTS

M. Legros would like to thank Dr. C. Bonnafos for helpful discussions about diffusion calculations.

REFERENCES

[1] I. Ames and F. d'Heurle, IBM J. Res. Develop. **14** 461 (1970).

[2] D. Gerth, D. Katzer, and R.A. Schwarzer, Phys. Stat. Sol (a) **146** 299 (1994).

[3] H.P. Longworth and C.V. Thompson, J. Appl. Phys. **69** 3929 (1991).

[4] P.A. Flinn, D.S. Gardner, and W.D. Nix, IEEE Trans. Electron. Dev. **34** 689 (1987).

[5] W.D. Nix, Metall. Trans. A **20A** 2217 (1989).

[6] P.R. Besser, S. Brennan, and J.C. Bravman, J. Mat. Res. **9** 13 (1994).

[7] J. Böhm, P. Gruber, R. Spolenak, A. Stierle, A. Wanner, and E. Arzt, Review of Scientific Instruments **75** 1110 (2004).

[8] O. Kraft, M. Hommel, and E. Arzt, Mat. Sci & Eng. A **288** 209 (2000).

[9] S. Bader, E.M. Kalaugher, and E. Arzt, Thin Solid Films **263** 175 (1995).

[10] G.J. Leusink, J.P. Lokker, M.J.C. van den Homberg, J.F. Jongste, T.G.M. Oosterlaken, G.C.A.M. Janssen, and S. Radelaar, Appl. Surf. Sci. **91** 215 (1995).

[11] J. Koike, S. Utsunomiya, Y. Shimoyama, K. Maruyama, and H. Oikawa, J. Mater Res. **13** 3256 (1998).

[12] A. Witrouw, J. Proost, P. Roussel, P. Cosemans, and K. Maex, J. Mater. Res. **14** 1246 (1999).

[13] D. Jawarani, H. Kawasaki, I.-S. Yeo, L. Rabenberg, J.P. Starck, and P.S. Ho, J. Appl. Phys. **82** 171 (1997).

[14] W.D. Nix, Scripta Mater. **39** 545 (1998).

[15] G. Dehm, T.J. Balk, H. Edongue, and E. Arzt, Microelectronic Engineering **70** 412 (2003).

[16] B. Kaouache, P. Gergaud, O. Thomas, O. Bostrom, and M. Legros, Microelectronic Engineering **70** 447 (2003).

[17] M. Legros, K.J. Hemker, A. Gouldstone, S. Suresh, R.M. Keller-Flaig, and E. Arzt, Acta Materialia **50** 3435 (2002).

[18] J.L. Bocquet, G. Brébec, and Y. Limoge, *Diffusion in metals and alloys*, in Physical Metallurgy, edited by R.W. Cahn and P. Haasen, (North Holland, Amsterdam, 1983).

[19] J.-P. Poirier, *Creep of crystals*. (Cambridge University Press, Cambridge, 1985).

[20] T.J. Balk, G. Dehm, and E. Arzt, Acta Materialia **51** 4471 (2003).

[21] H. Gao, L. Zhang, W.D. Nix, C.V. Thompson, and E. Arzt, Acta Materialia **47** 2865 (1999).

[22] D. Weiss, O. Kraft, and E. Arzt, Journal of Materials Research **17** 1363 (2002).

[23] A.B. Pandey, R.S. Mishra, A.G. Paradkar, and Y.R. Mahajan, Acta Materialia **45** 1297 (1997).

[24] T. Soga, K. Baskar, C.L. Shao, M. Umeno, T. Egawa, and T. Jimbo, Applied Surface Science **113-114** 573 (1997).

[25] P. Komninou, J. Stoemenos, G. Nouet, and T. Karakostas, Journal of Crystal Growth **203** 103 (1999).

[26] J.O. MacCaldin and H. Sankur, Appl. Phys Lett. **19** (1971).

[27] G.J. van Gurp, J. Apl. Phys **44** 2040 (1973).

[28] O. Bostrom, Wafer shape control - Study of the reactivity in Ti/Al dual layers and its effect on the stress. PhD thesis, Université d'Aix-Marseille III, Faculté des Sciences et Techniques de Saint-Jérôme (2001).

[29] R.W. Balluffi and A.V. Granato, *Dislocations, vacancies and interstitials*, in *Dislocations in solids*, edited by F.R.N. Nabarro, (North Holland, Amsterdam, 1979).

[30] J. Philibert, *Diffusion et transport de matière dans les solides*. (Editions de Physique, Paris, 1985), pp. 406-420.

[31] Y. Maeda, Phys. Rev. B **51** 1658 (1995).

[32] Y. Adda and J. Philibert, *La diffusion dans les solides - Tome II*. (Presses Universitaires de France, Paris, 1966).

[33] S.-I. Fujikawa, K.-I. Hirano, and Y. Fukushima, Metall. Trans. A **9** 1811 (1978).

[34] J. Mimkes, Thin Solid Films **25** 221 (1975).

[35] R.C. Picu and D. Zhang, Acta Materialia **52** 161 (2004).

[36] E. Ogris, A. Wahlen, H. Lüchinger, and P.J. Uggowitzer, J. Light Metals **2** 263 (2002).

[37] T.E. Volin, K.H. Lie, and R.W. Balluffi, Acta Met. **19** 263 (1971).

[38] M. Park, S.J. Krause, and S.R. Wilson, Applied Physics Letters **64** 721 (1994).

[39] R. Venkatraman, J.C. Bravman, W.D. Nix, P.W. Davies, P.A. Flinn, and D.B. Fraser, J. Electron. Mater. **19** 1231 (1990).

[40] M. Legros, Dehm, G. Balk, T. J. Arzt, E. Bostrom, O. Gergaud, P. Thomas, O. Kaouache, B. in *Multiscale Phenomena in Materials Experiments and Modeling Related to Mechanical Behavior* edited by H.M. Zbib, D.H. Lassila, L.E. Levine, and K.J. Hemker (Mater. Res. Soc. Symp. Proc., San Francisco, 2003), pp. 63-74.

Figure captions

Figure 1. TEM pictures taken in plane view samples of Al 1% Si 0.5% Cu film in the as deposited (a, b) and thermally cycled state (c,d). White arrows indicate Si precipitates. (a) and (b): bright and dark field micrographs images taken with g = $\underline{\bar{1}}11$ and g = $1\underline{\bar{3}}$, respectively. Images (c) and (d) were made with g = $\underline{\bar{2}}20$ and g = 022 respectively. Note the change in precipitate size between as-deposited (a, b) and cycled (c, d) films.

Figure 2. X-ray analysis in TEM nano-probe mode from two locations in the cross section sample of figure 3 (a) in a precipitate-free zone and (b) on a precipitate.

Figure 3. Cross-sectional TEM images of cycled Al(Si, Cu) films. (a), (b) and (c) are dark and bright field images taken with g = 111_{Si} and g = 131_{Si} of the precipitate and its corresponding stereographic projection. (d): dark field image of the twinned central region of the precipitate taken with g = $\underline{\bar{1}}1\underline{\bar{1}}_{SiTwin}$ (see stereographic projection in figure (e)). (f): dark field image of the surrounding Al grain made with g = $\underline{\bar{1}}11_{Al}$ (see stereographic projection in figure (g)). Corresponding diffraction patterns are enclosed in the top right corner of the micrographs.

Figure 4. *In situ* cross-sectional TEM experiment showing the interaction between dislocation 1 and two Si precipitates labeled A and C. Precipitate A dissolves rapidly

in favor of precipitate C through pipe-diffusion. Figure (g) is a sketch of the events seen in pictures (a) to (f). The small letters next to dislocation positions in figure (g) refer to pictures a to g. Thick arrows indicate the direction of motion of the dislocations. See text for details.

Figure 5. Evolution of the radii (a) and volumes (b) of precipitates A and C in function of time during the Si transfer from A to C. $V_C(t)$ and r_C (t) are calculated from r_A (t) under the assumption that V_C+V_A remains constant.

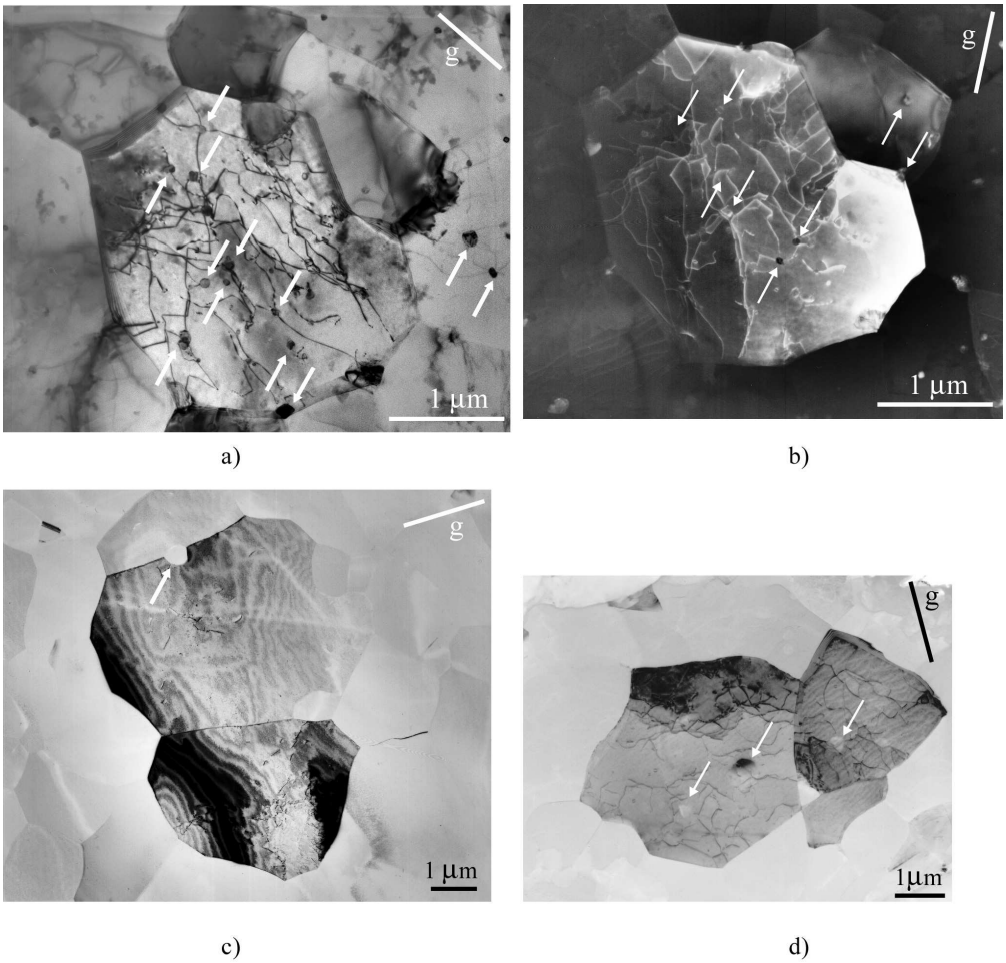

172x165mm (300 x 300 DPI)

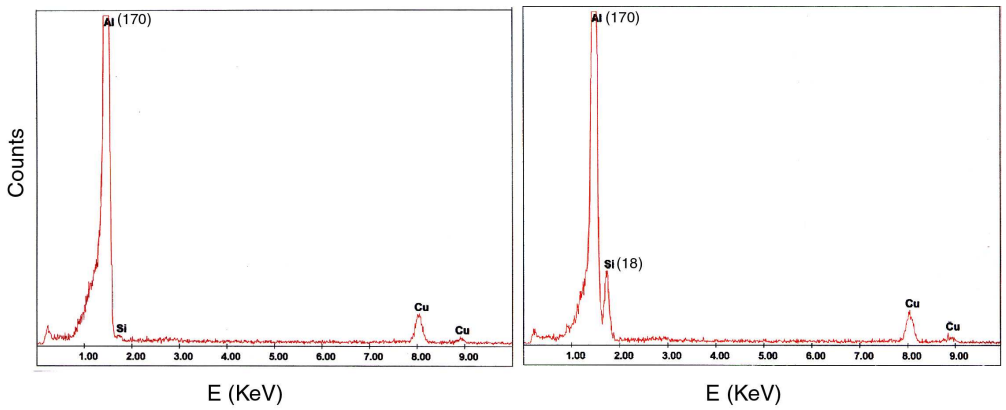

a) b)

191x89mm (300 x 300 DPI)

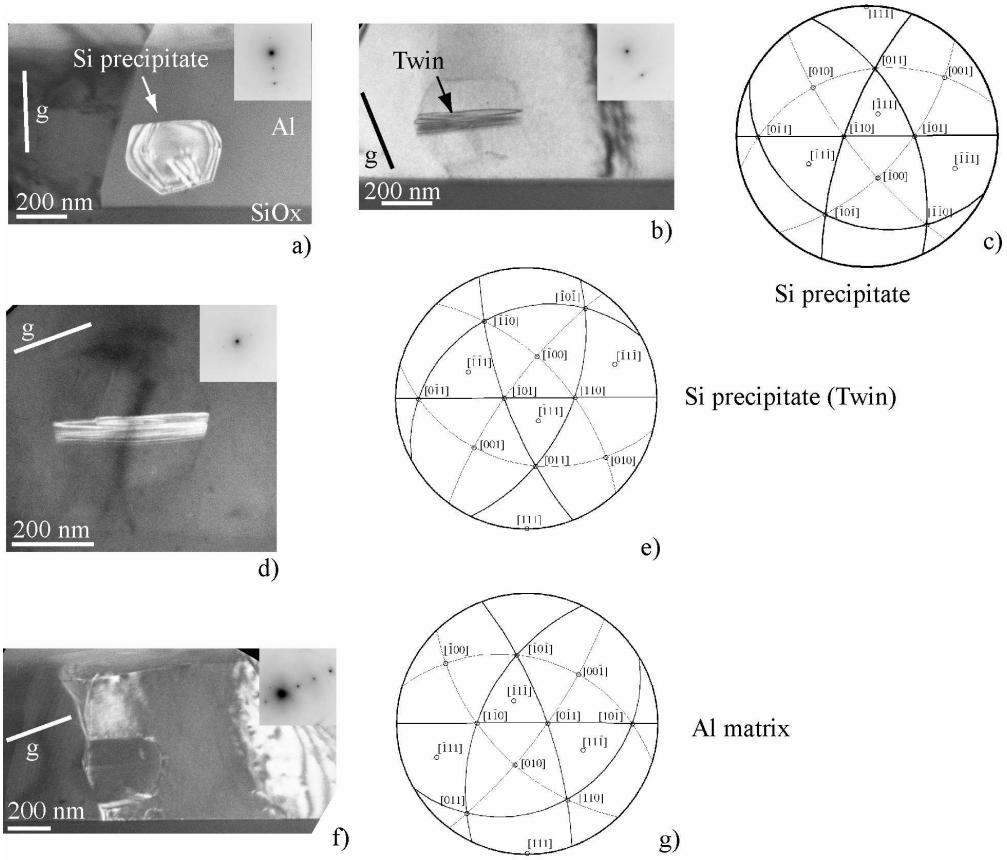

Figure 3

164x172mm (300 x 300 DPI)

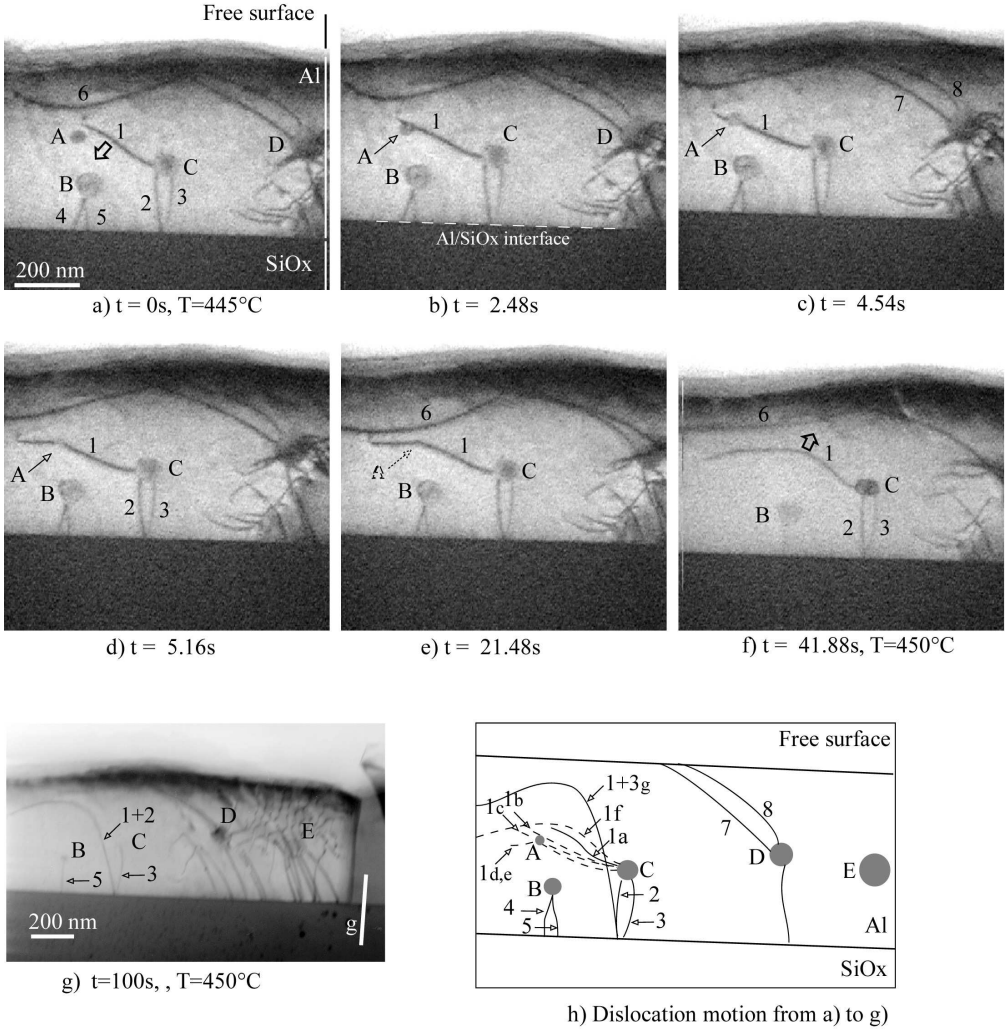

Fig. 4

186x201mm (300 x 300 DPI)

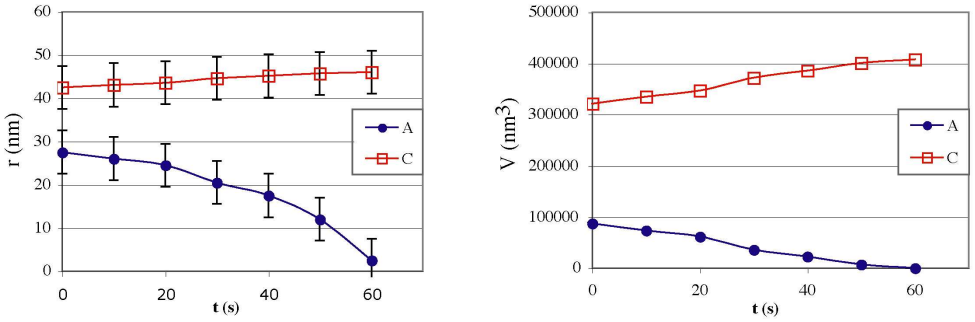

a) b)

figure 5

193x108mm (300 x 300 DPI)